

## ARTICLE OPEN



# Toward a circular economy: zero-waste manufacturing of carbon fiber-reinforced thermoplastic composites

Philip R. Barnett<sup>1,2,3,4</sup>✉, Nadim S. Hmeidat<sup>2,5</sup>, Bingqian Zheng<sup>4,6</sup> and Dayakar Penumadu<sup>2</sup>

Fiber-reinforced composites are becoming ubiquitous as a way of lightweighting in the wind, aerospace, and automotive industries, but current recycling technologies fall short of a circular economy. In this work, fiber-reinforced composites made of recycled carbon fiber and polyphenylene sulfide were recycled and remanufactured using common processing technologies such as compression and injection molding. An industrially viable size-exclusive sieving technique was used to retain fiber length and reduce variability in the mechanical properties of the remanufactured composites. Fiber length reduction alone could not explain the strength reductions apparent in the composites, which we propose are due to microstructural inhomogeneity as defined by poor dispersion of the fibers. Future recycling efforts must focus on fiber length retention and good dispersion to make composite remanufacturing a viable path toward a circular economy.

*npj Materials Sustainability* (2024)2:3 ; <https://doi.org/10.1038/s44296-024-00006-y>

## INTRODUCTION

Fiber-reinforced composites are the material of choice for aerospace and wind generation applications due to their low density, high strength and stiffness-to-weight, and excellent fatigue properties. Similar properties are desirable in the automotive industry. However, there are several key differences in the requirements of these industries. Unlike the commercial aviation industry, where capital expense is less important than operating cost, per unit cost plays a significant role in the decision-making process for automotive engineers. Similarly, the efficiency gains from larger wind turbine blades that necessitate the high stiffness of fiber-reinforced composites offset the increased material cost. The automotive consumer, however, is more cost-sensitive than in these more capital-intensive industries. Moreover, the end-of-life costs are of important consideration in the automotive industry due in part to legislation mandating recyclability. In the European Union, at least 95% of a vehicle's weight must be reused or recovered, with up to 10% being used for energy generation based on the End-of-Life Vehicle Directive<sup>1</sup>. This is a significant challenge for traditional continuous fiber-reinforced composites, as typical thermosetting matrices are not recyclable and make up between 25 and 45% of the mass of a structure. Even if the thermosetting matrix is burned for energy generation, it is still not possible to meet the 85% recyclability requirement. As such, there is a significant incentive for the automotive industry to consider thermoplastic matrix composites as an alternative to traditional thermosets.

Moreover, recycled carbon fiber stands to play an important role in the rapidly growing market for carbon fiber, which has experienced an 11.50 to 11.98% compound annual growth rate in the past decade<sup>2</sup>. As the use of carbon fiber in automotive structures continues to increase, there will likely be difficulties supplying enough virgin fiber to meet demand<sup>3</sup>. The market demands low-cost, low-embodied energy carbon fiber. Typical carbon fiber production consumes 55–165 kWh kg<sup>-1</sup> and costs on the order of \$33–66 per kg, but traditionally recycled carbon fiber

uses only 3–10 kWh kg<sup>-1</sup> and can be recovered for as little as \$5 per kg<sup>4,5</sup>. Moreover, recycled carbon fibers typically yield greater than 95% of their tensile strength and stiffness<sup>2</sup>. Given that as much as 40% of carbon fiber is currently sent to landfill as manufacturing waste<sup>5</sup>, there is significant value to recovering fibers for conversion into long fiber composites for the automotive industry.

The recycling of thermoplastic composite materials has received significant attention in recent years. The focus of recycling has been on recovering waste or end-of-life parts made of both discontinuous and continuous fiber composites. Injection molding provides for high throughput manufacturing, capable of producing on the order of millions of parts per year. As such, injection-molded composites have received some attention in the literature. Colucci et al.<sup>6</sup> recycled commercially available 30 wt% carbon fiber/polyamide 66 (PA66) injection-molded composites containing 0.3 mm carbon fibers. They found that the tensile strength decreased by about 20% after recycling, while the modulus decreased by about 10%. Pietroluongo et al.<sup>7</sup> recycled end-of-life radiator parts made of 35 wt% glass fiber/PA66 with a fiber length of about 0.3 mm and found that their tensile strength decreased by about 30% and the modulus by about 24%. Upon re-recycling, they found further decreases that were attributed to a reduction in fiber length during each injection molding step. Others have focused on integrating continuous fiber-reinforced thermoplastic grinds into injection molding compounds. Schinner et al.<sup>8</sup> integrated continuous carbon fiber/polyether ether ketone (PEEK) grind into neat PEEK injection molding compounds to yield a greater than 300% increase in tensile strength at 40 wt% fiber content and a greater than 1200% increase in modulus at 50 wt% fiber content. Despite these impressive improvements, the short fiber length leads to reduced strength relative to the theoretical maximum. To achieve the theoretical maximum strength of a composite, all fibers must be above the critical fiber length, which is the minimum fiber length required for a single fiber to break rather than be pulled out from the matrix when loaded in

<sup>1</sup>University of Tennessee-Oak Ridge Innovation Institute, Knoxville, TN, USA. <sup>2</sup>Tickle College of Engineering, University of Tennessee, Knoxville, TN, USA. <sup>3</sup>National Research Council Research Associateship Program, Air Force Research Laboratory, Wright-Patterson Air Force Base, OH, USA. <sup>4</sup>Air Force Research Laboratory, Wright-Patterson Air Force Base, OH, USA. <sup>5</sup>Manufacturing Science Division (MSD), Oak Ridge National Laboratory (ORNL), Knoxville, TN, USA. <sup>6</sup>UES, Inc, Dayton, OH, USA. <sup>✉</sup>email: pbarnet3@utk.edu

tension<sup>9</sup>. The critical fiber length is defined as:

$$L_c = \frac{\sigma_f r_f}{\tau_m} \quad (1)$$

where  $\sigma_f$  is the fiber strength,  $r_f$  is the fiber radius, and  $\tau_m$  is the fiber-matrix interfacial shear strength. For a typical carbon fiber/epoxy composite, the critical fiber length is on the order of several hundred micrometers but is significantly longer for thermoplastic composites with poorer interfacial strength.

Several authors have focused on preserving fiber length by creating compression molding compounds from thermoplastic composite scrap. Rather than degrade the fiber length through further compounding into injection molding pellets, the composite scrap is molded directly into a new part. Moothoo et al.<sup>10</sup> recycled E-glass/polypropylene woven composites cut into grains of various dimensions through compression molding. They found a significant strength reduction from the quasi-isotropic virgin laminate, achieving, at best 33% of the tensile strength and 88% of the tensile modulus. Vincent et al.<sup>11,12</sup> shredded carbon fiber/polyphenylene sulfide (PPS) waste to create a molding dough using a low-shear mixer. While they did not report mechanical properties, they described how sieving and varying the mixing parameters can be used to control fiber length and clustering. These two key parameters are expected to play an important role in maximizing the properties of recycled fiber-reinforced thermoplastics. Maintaining fiber length beyond the critical fiber length allows for the full fiber strength to be realized, and ensuring a homogenous distribution of the reinforcement reduces the stress-concentrating effects of agglomerates.

These key parameters are explored in the current work. Herein, recycled carbon fiber/PPS scrap material from organosheet composite manufacturing<sup>13</sup> has been recovered using a hammer mill. PPS is an engineering polymer capable of high-temperature operation with good chemical stability<sup>14</sup>. Waste material was gathered from prior manufacturing processes of carbon fiber/PPS composites, size reduced, and then sieved through 6.35 mm, #4 (4.75 mm), #8 (2.36 mm), #10 (2.0 mm), #20 (0.85 mm), and #40 (0.425 mm) screens to control the fiber length. The resulting particulate size distribution is shown in the Supplementary Section 1. Most of the recyclate was between 1 and 5 mm. Composites were manufactured from the recyclate using both compression and injection molding. The compression molded specimens were produced from either organosheets at 1 and 4 MPa molding pressure, hand-cut platelets of 12.7 mm × 12.7 mm planar dimensions, sieved recyclate, or wet laid (WL) mats consisting of the material atop the 6.35 mm sieve mixed with virgin fiber. A mixture of the #8, #20, and hand-cut platelets was also evaluated. Flat plaques were molded from which tensile specimens were extracted. Injection-molded specimens were produced from sieved material that was compounded with neat PPS. A commercial molding compound containing 50 wt% carbon fiber was used as a benchmark for the recycled injection-molded specimens. Neat PPS specimens were prepared using both compression and injection molding to serve as a control. The recycling process is shown schematically in Fig. 1, where waste material is milled into smaller particulates that are then molded into new parts that can later be recycled. The performance of the parts made of recyclate is strongly dependent on the fiber length, which is controlled by sieving. By controlling the distribution of fiber length in the recyclate molding compound, one can control the resulting performance.

The thermal and tensile properties of the composites were evaluated. The microstructure of the composites was studied using optical microscopy and scanning electron microscopy (SEM) to characterize the inhomogeneity of the composites produced using the different processes. This work demonstrates several key concepts for sustainable composites manufacturing:

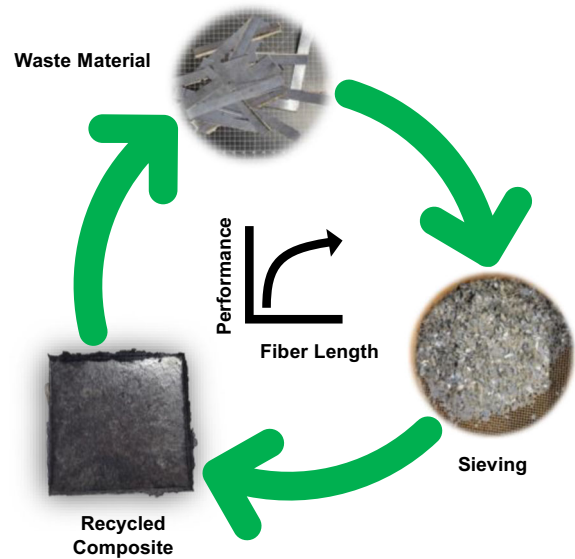


**Fig. 1 Controlled fiber length enables retained performance.** Controlling the fiber length by sieving recyclate allows for greater control of the performance of recycled products.

1. 100% material used by the recovery of waste material
2. Strength retention by control of the recyclate geometry and microstructural homogeneity using industrially viable processes
3. A reduction in remanufactured part variability
4. The use of previously recycled carbon fibers as a feedstock for new recycled composites

## RESULTS

### Thermal analysis

The thermal properties of the compression molded composite plates measured by differential scanning calorimetry (DSC) and thermogravimetric analysis (TGA) are summarized in Table 1. The crystalline percentage ( $X_c$ ) of the PPS matrix was significantly increased with the addition of carbon fibers, which serve to nucleate crystallites during cooling<sup>15</sup>. This resulted in a slight increase in the crystallization temperature ( $T_c$ ) of the composites relative to the neat PPS, as crystallization occurred more readily at the fiber/matrix interface. The melt temperature ( $T_m$ ) was unaffected by the presence of fibers. The 5% degradation temperature ( $T_{5\%}$ ) increased slightly with the addition of fibers, which serve to shield the PPS matrix from degradation. There also appears to be a strong molding pressure dependence on the  $T_{5\%}$ , with lower molding pressures yielding a smaller difference from the neat PPS. This is likely due to the higher crystalline content in the composites manufactured at higher molding pressures. The mass remaining after completion of the thermal sweep increased with molding pressure, indicating that higher fiber volume fraction was likely attained.

The thermal properties of the injection-molded composites are summarized in Table 2. The  $X_c$  was generally lower than achieved using compression molding, likely due to a change in cooling rate. The commercial compound was an exception, as it achieved the highest crystallinity of all specimens in this work. However, the grade of PPS used to make the commercial compound is not known. As a result, it is dubious to compare this result to the other samples in this work. The  $T_c$  was unaffected by the presence of fibers but was consistently higher than achieved from compression molding. Again, this is likely caused by a significant change in cooling rate during the molding process. The  $T_{5\%}$  did not vary significantly for the different injection-molded sample

**Table 1.** Thermal properties of compression molded specimens (sample size  $\geq 3$  specimens).

Material	$X_c$ (%)	$T_m$ (°C)	$T_c$ (°C)	$T_{5\%}$ (°C)	Mass remaining (%)
Neat PPS	39.7 $\pm$ 0.4	279.5 $\pm$ 0.6	223.5 $\pm$ 0.2	499.1 $\pm$ 2.7	50.5 $\pm$ 1.6
12.7 mm $\times$ 12.7 mm	47.0 $\pm$ 4.4	278.3 $\pm$ 0.4	225.5 $\pm$ 0.5	510.5 $\pm$ 1.4	75.9 $\pm$ 1.4
#8	54.8 $\pm$ 2.7	280.2 $\pm$ 0.3	228.7 $\pm$ 0.6	510.5 $\pm$ 0.7	74.4 $\pm$ 0.3
#20	50.5 $\pm$ 0.7	279.8 $\pm$ 0.3	228.6 $\pm$ 0.5	509.7 $\pm$ 1.6	72.3 $\pm$ 0.3
Mixed recyclate	49.5 $\pm$ 1.1	278.5 $\pm$ 0.5	227.8 $\pm$ 1.2	511.6 $\pm$ 1.3	75.0 $\pm$ 1.2
MD/CD 1 MPa	42.2 $\pm$ 3.7	278.2 $\pm$ 0.4	224.0 $\pm$ 0.6	500.0 $\pm$ 1.1	73.6 $\pm$ 0.5
MD/CD 4 MPa	45.8 $\pm$ 5.1	278.4 $\pm$ 0.6	224.2 $\pm$ 0.5	506.1 $\pm$ 4.5	77.8 $\pm$ 1.7
WL	40.4 $\pm$ 5.1	279.8 $\pm$ 0.3	223.8 $\pm$ 1.1	500.4 $\pm$ 2.3	73.1 $\pm$ 3.6

Error bounds represent one standard deviation.

**Table 2.** Thermal properties of injection-molded specimens (sample size  $\geq 3$  specimens).

Material	$X_c$ (%)	$T_m$ (°C)	$T_c$ (°C)	$T_{5\%}$ (°C)	Mass remaining (%)
Neat PPS	42.9 $\pm$ 0.4	282.6 $\pm$ 0.3	242.8 $\pm$ 0.3	508.1 $\pm$ 1.8	52.4 $\pm$ 0.7
Commercial	55.1 $\pm$ 1.4	283.0 $\pm$ 0.3	249.5 $\pm$ 0.2	511.1 $\pm$ 0.9	80.4 $\pm$ 0.5
#4	42.1 $\pm$ 4.0	281.0 $\pm$ 0.5	240.3 $\pm$ 1.0	507.0 $\pm$ 1.4	59.2 $\pm$ 1.8
#10	40.8 $\pm$ 3.4	281.0 $\pm$ 0.7	240.4 $\pm$ 0.1	508.8 $\pm$ 2.6	62.0 $\pm$ 1.9
#40	40.7 $\pm$ 2.0	280.8 $\pm$ 0.4	240.4 $\pm$ 0.3	507.0 $\pm$ 2.5	58.0 $\pm$ 0.6
<#40	40.7 $\pm$ 2.2	281.2 $\pm$ 0.8	240.5 $\pm$ 0.3	507.3 $\pm$ 1.3	62.0 $\pm$ 1.6

Error bounds represent one standard deviation.

formulations. The mass remaining for the commercial compound was significantly higher than all other specimens in this study. Compared to the compression molded samples, the fiber content of the injection-molded recyclate was significantly lower due to the mixing process required for extrusion of filaments for pelletization.

### Tensile testing of molded plates

The variability of recycled products is often viewed as one of their greatest limitations. This variability becomes even more significant for composites, which are by their nature a mixed waste stream. Here, we have shown that sieving serves to reduce variability for more consistent mechanical performance. The tensile properties of the compression molded plates are summarized in Fig. 2. In general, the tensile properties of the zero-waste plates were significantly lower than the organosheet plates. The organosheet plates were anisotropic, exhibiting varying properties in the machine (MD) and cross (CD) directions. The failure strain of the recycled composites decreased precipitously, which can likely be attributed to localized failure. Microstructural inhomogeneity may have allowed failure to initiate in matrix-rich regions at much lower loads than for homogeneous composites due to the lack of local reinforcement. This is supported by the observation that the failed specimens did not exhibit complete breakage in any of the zero-waste specimens, while the neat and organosheet specimens fully broke across the width of the samples into two pieces. As expected, the tensile modulus of the samples decreased with decreasing recyclate size. This is due to the reduced fiber length, which fails to adequately transfer load from the matrix to the fibers<sup>9</sup>. The insufficient load transfer to the shorter fibers is also expected to yield decreased tensile strength, which was also observed. Also of interest was the shift in the mechanical behavior of the composites. In general, the neat PPS and organosheets exhibited linear elastic behavior until failure. Surprisingly, the zero-waste samples exhibited significant plastic deformation that was

not apparent in even the neat polymer, as shown in Fig. 3. Such behavior points to localized failure prior to global ultimate failure.

Statistical analysis of the compression molded specimen tensile testing results shows that the strain-to-failure of many of the sample types within an individual group (e.g., particulate compounds, organosheets in MD and CD, WL) were not significantly different from each other. The  $p$  values are reported in a color-coded table in Fig. 4. Darker-colored boxes indicate that the  $p$  value is  $>0.05$ , with progressively lighter-colored boxes indicating smaller  $p$  values.  $P$  values  $<0.05$  indicate that the differences between samples are statistically significant to a 5% significance level. The strength of the particulate compounds was only significantly different for the larger 12.7 mm  $\times$  12.7 mm, with all the smaller compounds yielding similar strength. The modulus was more strongly influenced by the particulate size. As expected, the organosheets differed significantly depending on their orientation. The organosheets manufactured at higher pressures exhibited a slight, but statistically significant, decrease in strength for both directions and increase in modulus for those manufactured in the CD. The WL composite strength was significantly decreased at higher molding pressures and when using virgin fibers, whereas the modulus was only affected by the virgin fibers. The sizing present on the virgin fibers may have been incompatible with the PPS matrix.

In general, the expected trends are supported by the experimental data: the lower fiber volume fraction zero-waste composites yield lower mechanical properties, and the properties decrease with decreasing fiber length. The modulus of the mixed recyclate composites was well-predicted using a simple Rule of Mixtures based on the experimentally measured moduli for the 12.7 mm square, #8, and #20 recyclate plates:

$$E_c = \sum E_i W_i \quad (2)$$

where  $W_i$  corresponds to the weight and  $E_i$  the modulus of each component, respectively. For the mixed plate produced here, the predicted modulus is 16.6 GPa, which is only 3.6% different than

the measured 17.2 GPa. Unfortunately, the Rule of Mixtures does not predict the strength well for mixed composites, as evident from the decrease in strength and increase in variability for the mixed recycle relative to all the constituent components. Likewise, the strength of the wet-laid composites did not follow the anticipated trends. Despite their significantly longer fiber length and comparable fiber volume fraction, the strength of the wet-laid composites was on par with the sieved recycle.

The tensile properties of the injection-molded specimens are summarized in Fig. 5. Compared to the compression molding compounds, the injection-molded specimens achieved much higher tensile strength, with comparable tensile modulus. The reason for

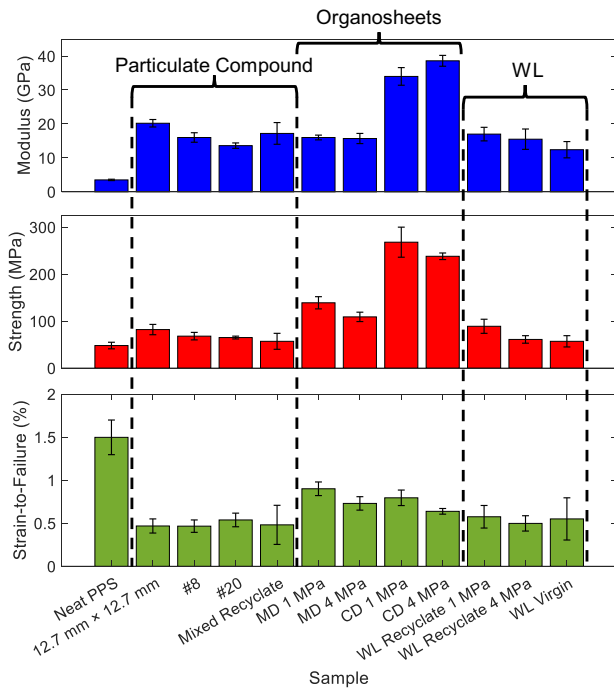


**Fig. 2 Tensile properties of compression molded composites.** Tensile modulus, strength, and strain-to-failure of compression molded composites is primarily impacted by fiber length (particulate compounds), fiber orientation (organosheets), and fiber dispersion (WL); error bars represent one standard deviation.

this increase in tensile strength is twofold: (1) the fibers were much more aligned in the flow direction during injection, and (2) a reduction in defects led to a significant increase in the strain-to-failure of the composites. Likewise, the injection-molded neat PPS yielded similar modulus to compression molding, but significantly increased strength and strain-to-failure. This change in strength may be attributed to the alignment of polymer chains during the injection molding process, whereas the compression molding process creates more random chain networks. The modulus of the commercial molding compound was significantly higher than that of the other injection-molded composites due to the much higher fiber volume fraction. However, this did not translate to an increase in the tensile strength, due in part to shorter fiber length and agglomerations of the reinforcing fibers that initiated localized failure, as shown by the significantly reduced strain-to-failure in Fig. 6.

Statistical analysis of the injection molding tensile testing results (Fig. 7) also shows that the strain-to-failure does not change significantly from sample to sample for the recycled fiber composites. The strain-to-failure of the recycled fiber composites was, however, significantly greater than that of the neat PPS. The tensile strength and modulus generally decreased with decreasing fiber length. The moduli of the #4 and #10 composites were not significantly different, although both have relatively similar fiber lengths in comparison to the finer sieves. This also manifested as statistically similar strengths for the #4 and #10 composites, as well as the #40 and material passing through the #40 sieve. One would expect the strength of these samples to be different if the only factors influencing their strength were the fiber length and orientation. This indicates that fiber dispersion likely plays a significant role in the strength reduction.

These results indicate that sieving is an effective way of producing recycled products with targeted properties. For example, products requiring lower stiffness and strength can be manufactured from shorter fibers, with the longer fibers being reserved for higher-performance products. This targeted recycling of composites would enhance their circularity, as longer fibers become shorter fibers in subsequent life cycles. Moreover, mixed composites demonstrate that the variability in mechanical properties can be reduced by size exclusion. Sieving is a mature process that can be readily implemented into existing recycling processes to yield higher-value recycled products.

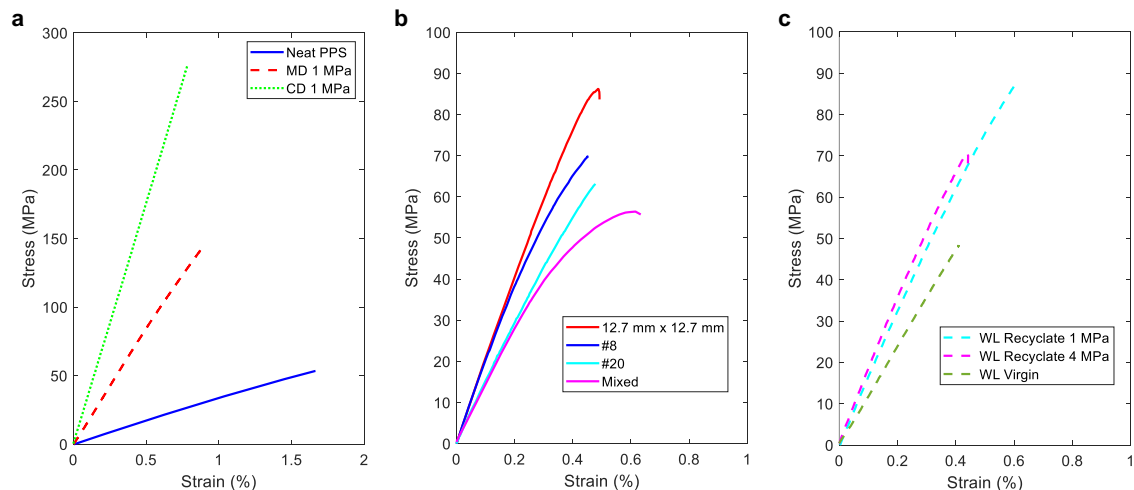


**Fig. 3 Stress-strain plots of compression molded composites.** Representative tensile plots of organosheet composites (a), particulate molding compounds (b), and wet laid composites (c) represent significant differences in strength and stiffness due to differences in fiber orientation, fiber length, and fiber volume fraction.

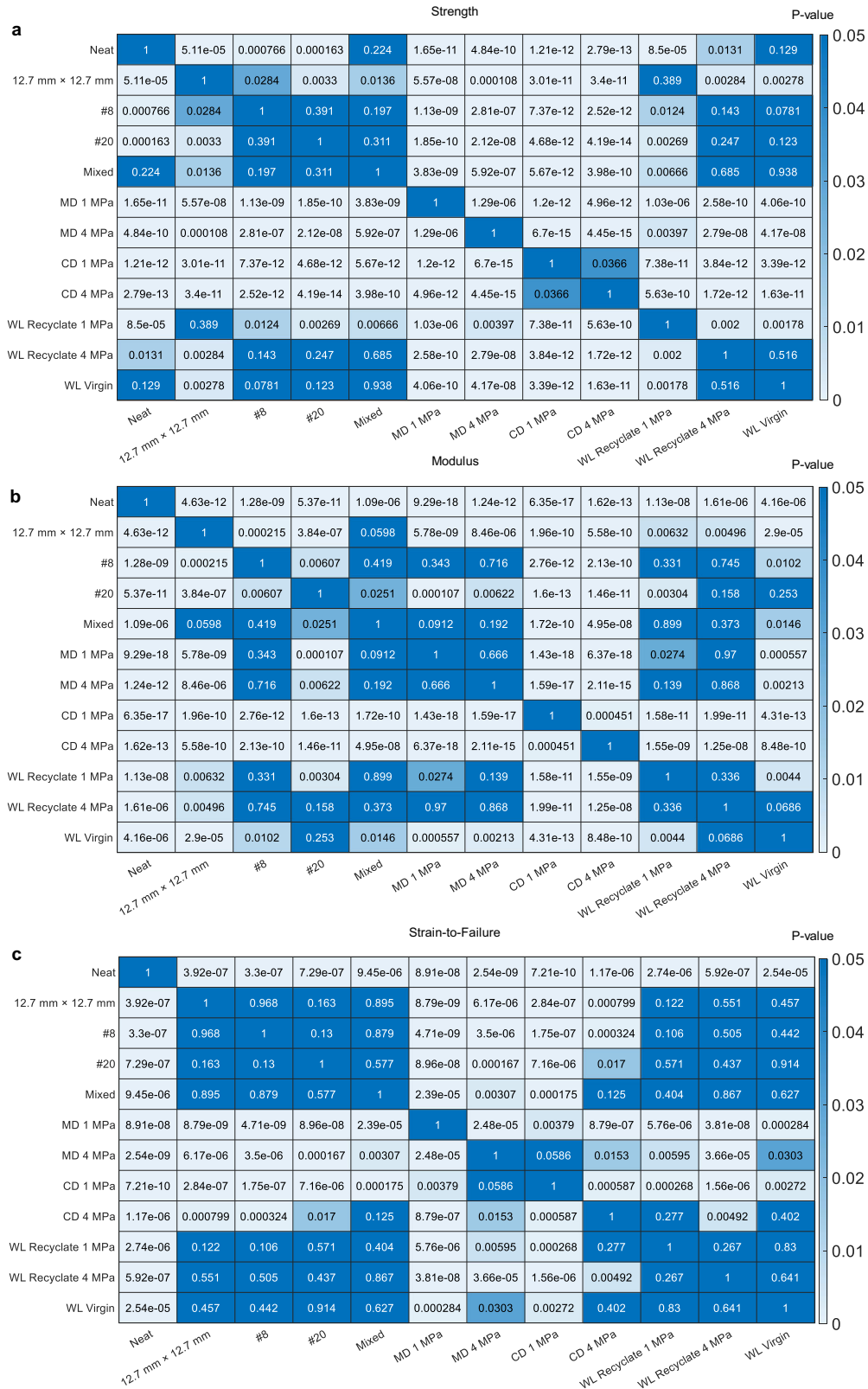


**Fig. 4 Statistical analysis of compression molded composite properties.** P values for differences in strength (a), modulus (b), and strain-to-failure (c) for compression molded composites where values below 0.05 indicate statistically significant differences between samples.

**Microstructure evaluation**

In general, the zero-waste molded composites were well-consolidated. As shown in Table 3, the void content measured via

optical microscopy was well below 1% for each of the composites produced from sieved material. Conversely, the organosheet and wet-laid composites exhibited higher void content, likely due to a

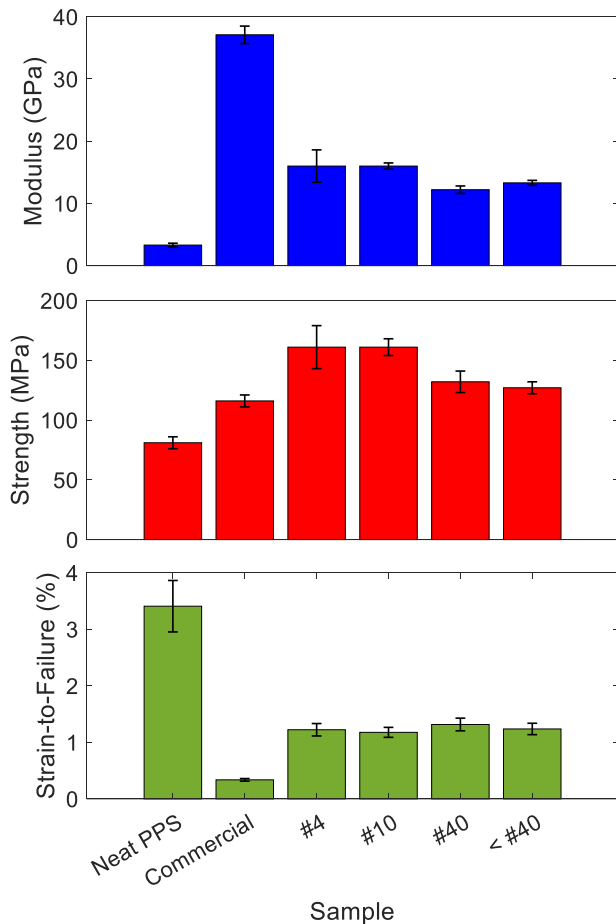


**Fig. 5 Tensile properties of injection molded composites.** Tensile modulus, strength, and strain-to-failure of injection molded composites are impacted by fiber volume fraction and fiber length; error bars represent one standard deviation.

combination of reduced molding pressure and greater fiber length that inhibited polymer flow. The mean fiber length (more details in Supplementary Section 2) decreased with a decrease in sieve dimensions. Additional details on the fiber volume fraction can be found in the Supplementary Section 3. Furthermore, the fiber volume fraction of the organosheet composites measured by image analysis was higher than achieved in the recycle. This result is likely due to edge effects in the scrap material used to produce the zero-waste compression molded composites. The organosheet composites were cut from the middle of the organosheets, which contain largely homogeneous fiber and matrix content. However, at the edges, there exists some regions of dry fiber and others of neat matrix. During the sieving process, most of the dry fiber remained on top of the 6.35 mm mesh, while the smaller neat resin portions fell through smaller sieves. For example, the decrease in the fiber volume fraction of the #20 recycle samples can be attributed to the sieving process itself, in which more neat PPS particulates were present than in the #8 recycle (see Supplementary Fig. 3). As a result, the fiber volume fraction of the sieved material was reduced relative to the organosheet composites. The fiber volume fraction of the injection-molded samples was significantly reduced from the organosheets due to the addition of 50 wt% neat PPS to the recycle molding compound.

The dispersion index (DI), a measure of the fiber spacing compared to the ideally homogeneous composite, provides a unique insight into the strength variability measured in this work. The organosheet composites exhibited less microstructural

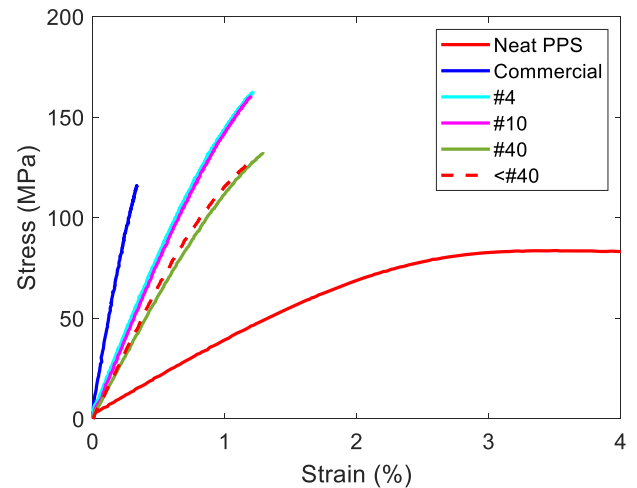


**Fig. 6 Stress-strain plots of injection molded composites.** Representative tensile plots of all injection molded composites tested demonstrate significant differences in strength and stiffness due to fiber length and fiber volume fraction.

variability than the compression molded recycle, as evident from their lower DI. The strength for the #8, #20, and mixed recycle decreased with an increase in DI, indicating that poor dispersion of the fibers led to a decrease in strength. The 12.7 mm × 12.7 mm samples exhibited a higher DI than the #8 and #20 recycle but still achieved higher strength. This increase in strength can be attributed to the fiber length, which was much longer than for the hammer-milled material. As a result, this indicates that increasing fiber length can help to offset agglomeration stress concentrations. The DI for the wet-laid composites was significantly higher than for any of the other compression or injection-molded composites. This is due to poor dispersion of the virgin chopped fiber bundles—the virgin wet-laid composites yielded the highest DI. The dispersion of the injection-molded composites was comparable to the compression-molded nonwovens and generally better than the recycle compression molding compound. Decreasing fiber length generally led to improved dispersion, apart from the commercial compound containing a much higher fiber volume fraction. However, the improved dispersion came at the cost of a greater proportion of fibers being below the critical length. As a result, the strength of the injection-molded specimens illustrates the competing influence of fiber length and dispersion.

It is clear from the larger variability in fiber volume fraction of the compression molded specimens that their microstructure is less homogeneous. Moreover, SEM imaging of failed compression molded tensile specimens in Fig. 8 revealed increasingly large matrix-rich regions as the particle size decreased. The largest matrix-rich regions appeared in the wet-laid virgin fiber composites. The fiber bundles failed to properly disperse, resulting in regions of extremely high fiber content surrounded by matrix with nearly no reinforcement. Despite similar fiber volume fraction to the original organosheets and fibers significantly longer than the critical length, the strength was dramatically reduced. As such, the inhomogeneity of the zero-waste compression molded composites can largely be blamed for their reduced performance.

The injection-molded samples present a unique trend. The modulus is strongly dependent on the fiber volume fraction, whereas the strength is more nuanced. Most of the fibers are aligned in the tensile direction. As the size of the recycle decreases, the prevalence of fiber pull-out increases, indicating that more fibers were below the critical length (see Supplementary Section 4). In the authors' prior work<sup>16</sup>, the fiber-matrix interfacial shear strength was determined to be 14.16 MPa ± 2.96 MPa, and

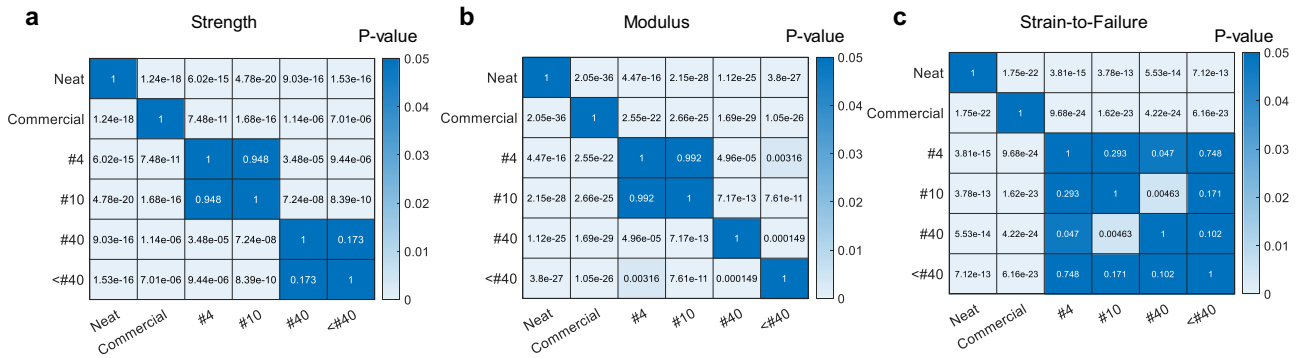


**Fig. 7** Statistical analysis of injection molded composite properties. *P* values for differences in strength (a), modulus (b), and strain-to-failure (c) for compression molded composites where values below 0.05 indicate statistically significant differences between samples.

**Table 3.** Microstructural properties of the composite influencing strength (sample size  $\geq 3$  specimens).

Material	Fiber volume fraction (%)	Dispersion index (unitless)	Mean fiber length ( $\mu\text{m}$ )	Void volume fraction (%)	Strength (MPa)
12.7 mm $\times$ 12.7 mm	$36.7 \pm 2.3$	$2.922 \pm 0.240$	965.1	$0.3 \pm 0.2$	$82 \pm 11$
#8	$30.7 \pm 2.0$	$2.777 \pm 0.265$	861.3	$0.2 \pm 0.1$	$68 \pm 8$
#20	$28.9 \pm 2.9$	$2.867 \pm 0.220$	488.5	$0.3 \pm 0.3$	$65 \pm 3$
Mixed recycle	$30.3 \pm 3.1$	$2.949 \pm 0.067$	788.3	$0.2 \pm 0.1$	$57 \pm 17$
1 MPa*	$28.8 \pm 2.2$	$2.691 \pm 0.376$	>1000	$4.3 \pm 3.8$	$139 \pm 13$ (MD) $268 \pm 32$ (CD)
4 MPa	$36.0 \pm 5.4$	$2.637 \pm 0.228$	>1000	$6.1 \pm 6.3$	$109 \pm 10$ (MD) $238 \pm 7$ (CD)
WL recycle 1 MPa	$27.0 \pm 6.4$	$3.812 \pm 0.814$	>1000	$3.5 \pm 2.2$	$89 \pm 15$
WL recycle 4 MPa	$31.3 \pm 9.6$	$3.809 \pm 0.291$	>1000	$3.8 \pm 3.1$	$61 \pm 8$
WL virgin	$25.1 \pm 3.8$	$6.940 \pm 1.121$	>1000	$2.5 \pm 2.4$	$57 \pm 12$
Commercial	$35.9 \pm 0.9$	$2.987 \pm 0.126$	135.3	$0.1 \pm 0.0$	$116 \pm 5$
#4	$11.9 \pm 1.5$	$2.871 \pm 0.041$	270.4	$0.4 \pm 0.1$	$161 \pm 18$
#10	$11.4 \pm 0.2$	$2.809 \pm 0.082$	251.4	$0.7 \pm 0.2$	$161 \pm 7$
#40	$9.2 \pm 0.1$	$2.526 \pm 0.102$	183.4	$0.6 \pm 0.3$	$132 \pm 9$
<#40	$12.9 \pm 0.3$	$2.654 \pm 0.066$	127.9	$1.0 \pm 0.2$	$127 \pm 5$

\*From the authors' prior work<sup>13</sup>; Error bounds represent one standard deviation.

the fiber diameter was  $7.3 \mu\text{m} \pm 0.23 \mu\text{m}$ . This yields a critical fiber length of  $1141 \mu\text{m}$ , which is larger than the #20 sieve dimensions. This means that particulates that passed through sieves smaller than this (i.e., samples labeled #40 and <#40) only contain fibers shorter than the critical length and are expected to exhibit fiber pull-out as the primary failure mode. The expected behavior is shown from the increased fiber pull-out in the SEM imaging shown in Fig. 9, explaining the reduction in tensile strength of the fine particulate composites.

## DISCUSSION

Carbon fibers generally make up most of the material costs for carbon fiber-reinforced polymers, due in large part to the energy required for their manufacture. At a typical cost of \$33–66 per kg<sup>5</sup>, and assuming a conservative 30% scrap rate, as much as \$10–20 per kg of virgin carbon fiber value is currently lost as manufacturing waste. For economic viability, the cost of recovery must be below this range, including the savings associated with landfill avoidance. The energy required for mechanical recycling of composites ranges from 0.03–1.33 kWh per kg<sup>3</sup>. The August 2023 United States industrial electricity cost was \$0.0882 per kWh<sup>17</sup>, yielding a hammer milling cost between \$0.0025 and 0.1173 per kg of mechanically recycled material, excluding labor and capital

expenditures. The energy usage for sieving and washing is not well-established but is expected to be similar. The labor cost for recovering carbon fiber from automotive waste is estimated at \$1.71 per kg<sup>5</sup>, making up the majority of the cost of recycling. Transportation costs are expected to be on the order of the recycling energy costs, a small portion of the total costs<sup>5</sup>. The resulting total costs of recycling are likely to be economical for carbon fiber if the logistics are in place for efficient collection. From a technology readiness perspective, mechanical grinding of carbon fiber composites has been identified to be at the demonstration stage<sup>18</sup>, which is below other waste management techniques such as pyrolysis and landfill. This may be partially attributed to the relatively lower value of fibers with severely reduced length. This is less of a problem for fibers recovered by pyrolysis processes that can routinely recover fibers greater than 10 mm in length but require substantially more energy (2.9–9.9 kWh per kg or \$0.26–0.87 per kg) and release carbon dioxide into the atmosphere. Size exclusion by sieving is a low-energy process that can be used to improve the mechanical properties of mechanically recycled fiber composites, which may make this a more viable alternative recycling strategy.

The development of a circular economy for fiber-reinforced composites must consider how their performance benefits can be retained in subsequent lives. This requires important

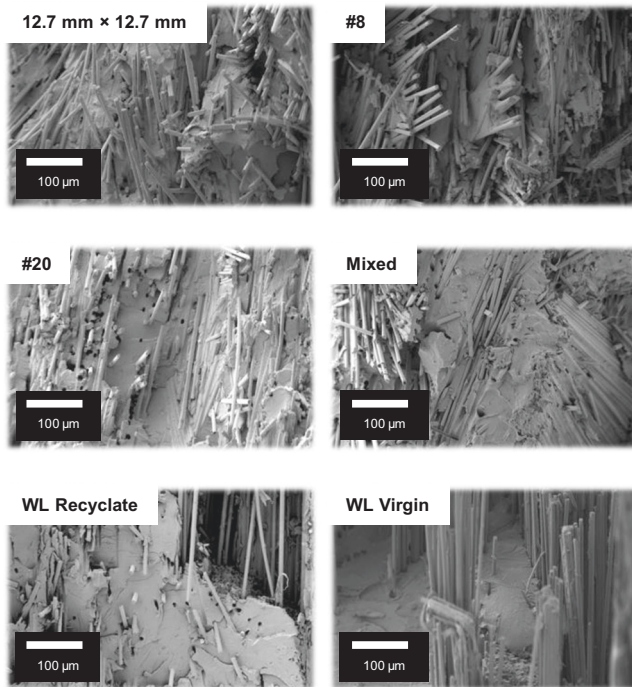


**Fig. 8 SEM images of failure surfaces of compression molded composites.** Local inhomogeneity is increasingly worse for mixed and wet laid composites.

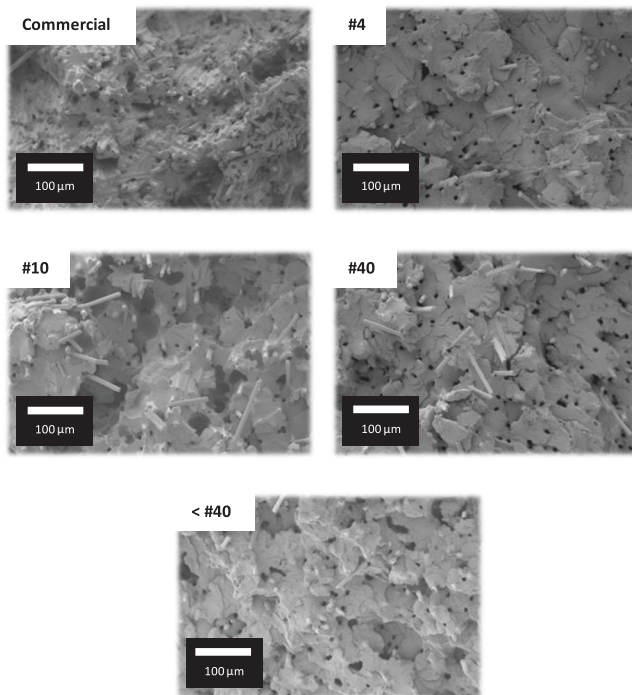


**Fig. 9 SEM images of failure surfaces of injection molded composites.** Increasing prevalence of fiber pull outs indicates increasing number of fibers below the critical fiber length.

considerations regarding fiber length retention and material homogeneity. Here, we have shown that the strength and stiffness of recycled fiber-reinforced composites are strongly influenced by both. The fiber length primarily influenced the modulus, which was also strongly dependent on the fiber orientation. The strength was moderately influenced by fiber

length for randomly oriented compression-molded specimens, but more strongly influenced by fiber length in highly aligned injection-molded composites. Inhomogeneity also played a significant role in the strength of the composites, where poor dispersion led to a significant strength reduction.

The variability of recycled products is often one of their most difficult limitations to overcome. This is even more significant for fiber-reinforced composites, as these materials contain inherently mixed waste streams. We successfully reduced the variability of recycled composites by size exclusion. While sieving may be an industrially viable solution to reducing variability, it does not offer a solution to fiber length retention. Larger recyclate may again be recycled into smaller pieces, but the fiber length will eventually become untenable, ending circularity. This work illustrates the need for the development of new recycling and remanufacturing technologies for fiber-reinforced composites. Such technologies should focus on retaining fiber length at each product cycle, aligning fibers during remanufacture, and ensuring homogeneous dispersion of the fibers in remanufactured products. As composites become more ubiquitous in the wind, aerospace, and automotive industries, it is imperative that such technologies be developed to ensure that we do not trade short-term efficiency gains for long-term waste generation.

## METHODS

### Materials

Recycled carbon fibers in the form of a carded nonwoven preform were provided by Gen 2 Carbon. From earlier work, the nonwoven areal density was  $184.2 \pm 11.2 \text{ gm}^{-2}$ , made of  $38.8 \text{ mm} \pm 22.2 \text{ mm}$  long fibers with strength and modulus of  $4426 \pm 386 \text{ MPa}$  and  $206 \pm 14 \text{ GPa}$ , respectively<sup>16</sup>. The recycled fibers were recovered using a commercial pyrolysis process and manufactured into preforms exhibiting mild anisotropy in the cross-direction of the roll product. This roughly 2:1 orientation was induced by the cross-lapping process used to build thickness in the carded preforms<sup>13</sup>. Precision chopped virgin carbon fibers of 12 mm length with 4150 MPa tensile strength and 230 to 255 GPa modulus containing sizing of less than 2 wt% were provided by Gen 2 Carbon. Compared to the recycled fibers, the tensile strength is slightly lower and the modulus slightly higher.

PPS films were purchased from CS Hyde (Solvay, Ryton QC160P). The nominal film thickness was 0.127 mm, and the density was  $1.34 \text{ g cm}^{-3}$ , indicating that the films were highly amorphous. The films were used to manufacture organosheets, as described in the following section. PPS pellets (Solvay, Ryton QA200P) were acquired for the preparation of injection molding compounds. The physical and mechanical properties of these two grades of PPS are nearly equivalent based on the manufacturer-supplied datasheets. A commercial molding compound containing 50 wt% carbon fiber content that was developed for material extrusion 3D printing (Electrafil PPS CF50 3DP, TechmerPM) was studied for comparison to recycled injection-molded composites.

### Organosheet composite manufacturing

Organosheets were produced in accordance with the authors' prior work<sup>13</sup> by sandwiching a recycled carbon fiber preform (Fig. 10) between two PPS films and then compression molding at 300 °C and 1 MPa pressure for 5 minutes, followed by cooling under pressure in a heated laboratory press (Carver, model 3895). Kapton release films coated with a release agent (Loctite, Frekote 800NC) were used to prevent the composite from sticking to flat aluminum molding plates. The 250 mm × 250 mm organosheets were then cut to 100 mm × 100 mm squares and placed in a closed-wall aluminum mold coated with release agent. Molding was completed at 300 °C and 1 MPa pressure for 5 minutes, followed by cooling to at least 60 °C under pressure, to produce a



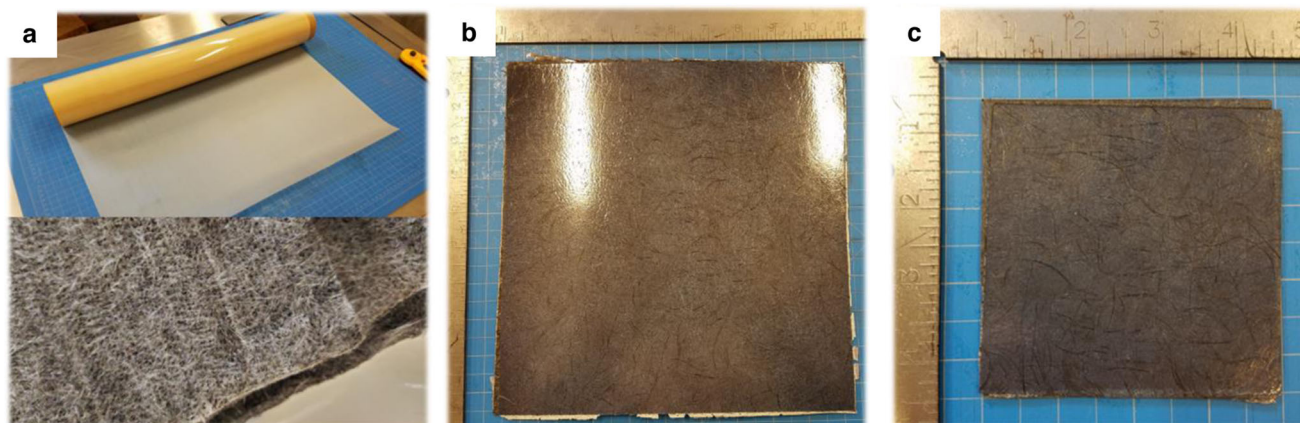


**Fig. 10** Manufacturing process for organosheet composites. PPS matrix films and fiber preforms (a) are layered and compression molded to form organosheets (b) that are stacked and compression molded to manufacture organosheet composites (c).

plate of approximately 2 mm thickness. To evaluate the influence of molding pressure, samples were also produced at 4 MPa using the same temperature and time profiles. The remaining scrap material, roughly 36% of the original organosheets, was retained for recycling.

#### Waste material preparation

Waste organosheet size reduction was accomplished by either hand cutting with scissors or size reduction in a hammer mill (PelletMasters, Model CF198). 12.7 mm × 12.7 mm squares were hand-cut from the scrap material to produce a well-defined chip size for the production of a zero-waste molding compound. Hammer-milled material was gathered and then sieved through 6.35 mm, #4 (4.75 mm), #8 (2.36 mm), #10 (2.0 mm), #20 (0.85 mm), and #40 (0.425 mm) screens (Gilson Company, Model SS-R). Due to the large volume of dry fiber apparent in the recyclate, sieving was performed in two increments of five minutes each. After the first increment, the material in the top sieve was flipped over to allow any trapped consolidated particles to fall through the mesh during the second shaking cycle. The resulting particulate size distribution is shown in Supplementary Fig. 5. Most of the recyclate was between 1 and 5 mm.

After sieving, contaminants in the material were removed by placing it in a water bath containing a small amount of commercial surfactant (Air Products, Tomamine AO-14-2). This allowed the primarily bio-based contaminants from the hammer mill to float, as the denser fibers and composite sunk. The floating material was skimmed off the water surface, and then the recyclate was thoroughly washed in a #325 sieve (45 μm) with tap water until all bubbles were gone to remove any residual surfactant. Then, the recyclate was dried in a vacuum oven for a minimum of four hours at 100 °C prior to processing. Images of the steps in the recycling and remanufacturing process can be found in Supplementary Section 1.

#### Zero-waste molding compound manufacturing

The sieved material was used as a molding compound to produce 100 mm × 100 mm plates using the mold described earlier. A plate thickness of 2 mm was targeted, but high flash led to thickness reductions in some samples. Molding pressure was set to 5 MPa to allow for good consolidation, as initial trials showed poor consolidation from plates molded at 1 MPa due to poor material flow. To examine the impact of recyclate size, plates were made from 12.7 mm square platelets and material that passed through the #8 and #20 sieves (Fig. 11). An additional plate was made from mixed recyclate, consisting of equal parts #8, #20, and 12.7 mm square platelets. To provide a baseline, a neat PPS plate was

molded by stacking films to form a plate from which tensile bars were cut.

The material from #4, #10, #40, and the material passing through the #40 sieve was used to produce an injection molding compound (Fig. 12). Mixtures of neat PPS pellets, and recyclate were prepared at a 1:1 weight ratio. Mixing was done mechanically in a single screw filament extruder (Filabot EX2, Filabot) using a 3 mm nozzle size at a constant temperature of 300 °C for all mixtures. To accelerate cooling of the extruded filaments, a fan was placed ~20 cm from the extrusion nozzle. Prior to extrusion, the mixtures were vacuum dried at 80 °C for 2 hours to remove any moisture. The extruded filament could not be spooled due to its high stiffness and was therefore recovered in straight sections of limited length (typically <300 mm). The extruded filament was then pelletized using a filament chopper (Filabot Pelletizer, Filabot). The pellets were then used to mold ASTM D638 type V dogbone samples using a benchtop injection molding machine (HAAKE MiniJet Pro, ThermoFisher Scientific). Prior to injection molding, the pellets were dried in a convection oven at 150 °C for 3 hours. Injection molding was completed at 305 °C for the neat PPS and 315 °C for the composites. The mold temperature was held at 149 °C for all samples. The injection pressure was 693 bar for 2 seconds, followed by a 672 bar compaction hold for 2 seconds. A commercial molding compound containing 50 wt% carbon fiber was used as a benchmark for the recycled injection-molded specimens. Neat PPS specimens were prepared to serve as a control.

The material failing to pass through the 6.35 mm sieve was processed using a wet laid (WL) process. This modified papermaking process involves producing a slurry of fibers in an aqueous suspension, followed by draining and drying to form a nonwoven preform suitable for compression molding (Fig. 13). Due to the difficulty of processing the recyclate; it was mixed in a 1:4 ratio by fiber mass with precision chopped carbon fibers to yield composites with similar fiber volume fraction to the compression molding compounds. Nonwoven mats of 305 mm × 305 mm and  $302.3 \pm 0.7 \text{ gm}^{-2}$  were manufactured by mixing in a Thwing-Albert tank filled with 20 L of water held at 40 °C for 20 minutes using the mixer design described by Ghossein<sup>19</sup>. To aid in dispersion, 4 g each of alkyl amine surfactant (Nalco 8493) and anionic flocculent (Nalclear 7768) were added to the mixture. The WL mats were then dried at 104 °C for 30 minutes. The dried mats were placed between 0.127 mm PPS films and compression molded using the same parameters as the carded nonwovens. The pressure was either 1 MPa or 4 MPa, allowing for a direct comparison to the initial material. This process is known to produce parts exhibiting in-plane isotropy, so testing at different orientations was not considered. For

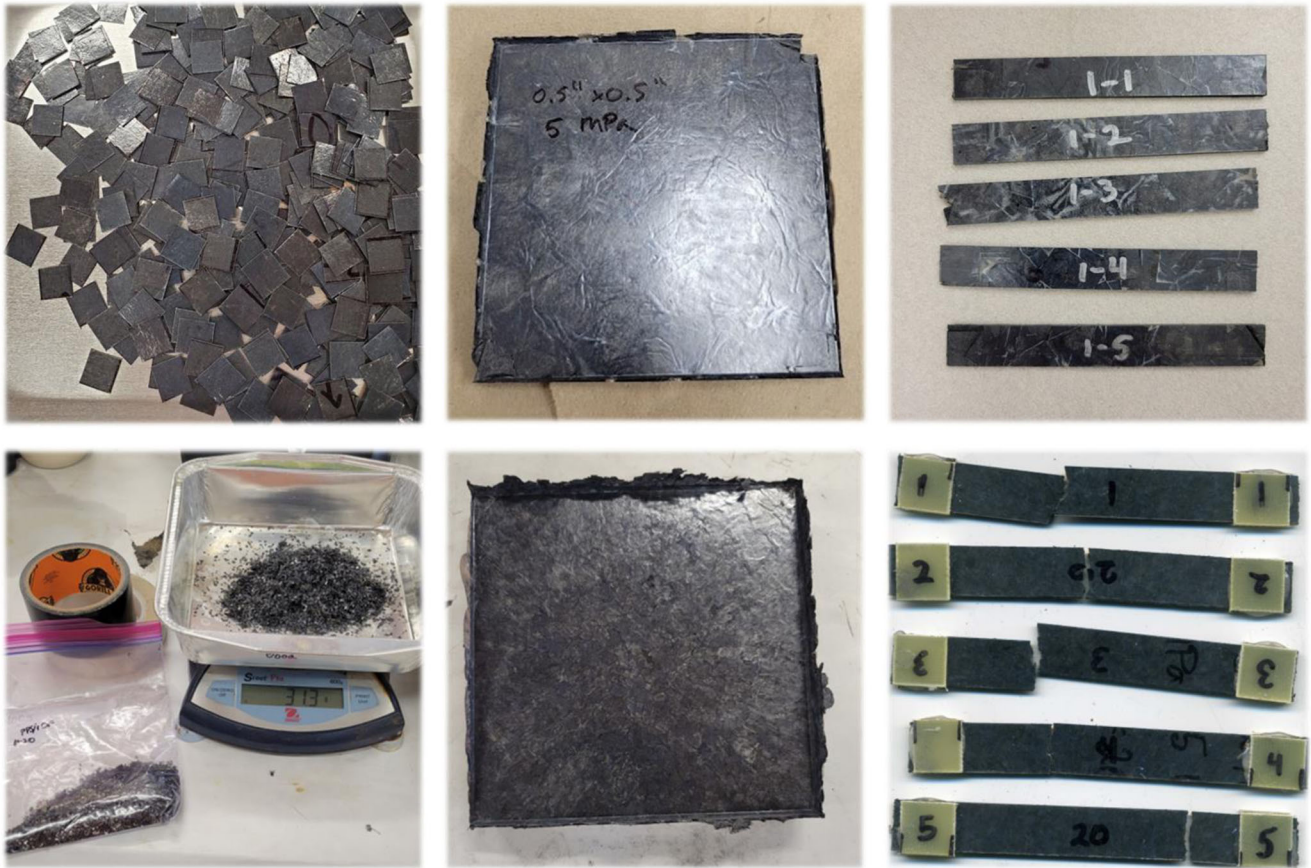


**Fig. 11 Manufacturing process for particulate composites.** 12.7 × 12.7 mm recyclate (top) and #20 molding compound (bottom) are compression molded into plates from which tensile specimens are extracted.

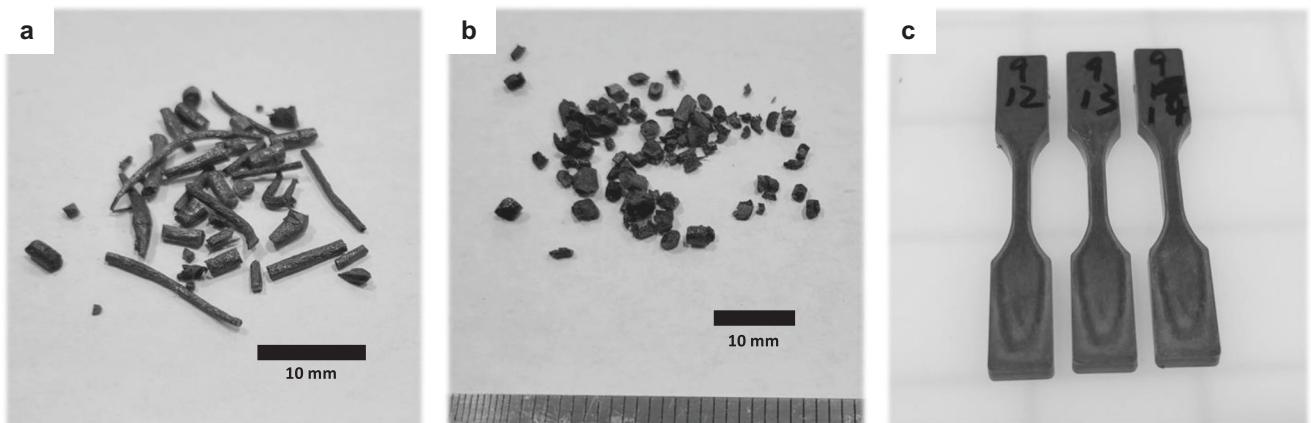


**Fig. 12 Manufacturing process for injection molded composites.** Recyclate (a) and commercial (b) injection molding compounds are used to produce tensile specimens (c).

comparison to the recycled composites, a nonwoven made entirely of precision chopped carbon fiber with an areal density of 184 g m<sup>-2</sup> was produced and molded at 1 MPa pressure.

### Thermal analysis methods

DSC and TGA were used to evaluate the specimens. DSC samples were heated from 25 to 325 °C and then cooled back to 25 °C at 10 °C min<sup>-1</sup> (DSC 2500, TA Instruments). The resulting thermograms were analyzed to determine the crystalline percentage of

the PPS matrix using a rule of mixtures modification:

$$X_c(\% \text{ crystallinity}) = \frac{\Delta H_m + \Delta H_c}{\Delta H_f(1 - W_f)} \quad (3)$$

where  $\Delta H_m$  is the endothermic enthalpy of melting,  $\Delta H_c$  is the exothermic enthalpy of crystallization,  $\Delta H_f$  is the endothermic enthalpy of fusion for the crystalline phase, and  $W_f$  is the weight fraction of fibers in the sample that do not contribute to the measurement. The 100% crystalline enthalpy of fusion for PPS is not well-defined and varies as a function of processing history<sup>20</sup>,

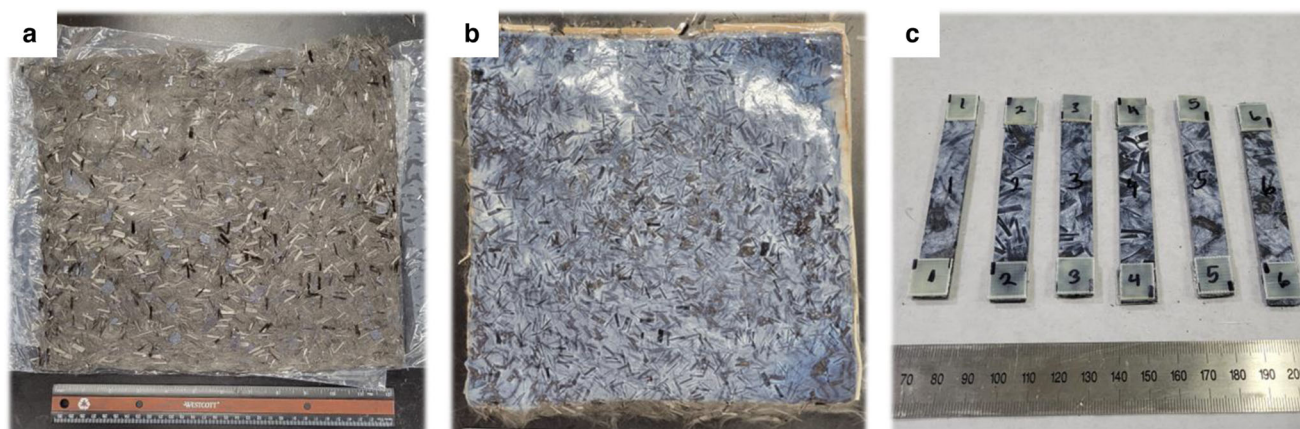


**Fig. 13 Manufacturing process for wet laid composites.** Wet laid preforms (a) are consolidated into organosheets (b) using compression molding and stacked and molded to form composites (c).

ranging from 50 to 150.4 J g<sup>-1</sup>. In the authors' prior work, the 100% crystalline enthalpy of fusion was found to be 88.37 J g<sup>-1</sup>, which is the value used in this work. The melting temperature ( $T_m$ ) and recrystallization temperature ( $T_C$ ) were reported as the peak of the melt endotherm and the peak of the crystallization exotherm during cooling, respectively. The samples and pan were then transferred for thermogravimetric analysis.

The weight fraction of fibers in the DSC samples was determined through TGA. Samples of 12.2 ± 2.5 mg were heated in nitrogen from room temperature to 600 °C at 10 °C min<sup>-1</sup> (TGA 550, TA Instruments). The samples were inside aluminum DSC pans containing a pinhole to allow trapped gases to escape, whose mass loss in this range was negligible. The 5% degradation temperature ( $T_{5\%}$ ) was recorded, as well as the mass percent remaining at 600 °C. Fiber length was measured from optical micrographs of larger composite specimens that were pyrolyzed in a box furnace to remove the matrix. At least 2000 fibers per sample type were measured. More details can be found in the Supplementary Section 2.

### Tensile testing methods

Tensile testing of the molded specimens was completed according to the ASTM D3039 standard. Additional details are available in the Supplementary Section 5. Straight-sided specimens of 12.7 mm width and 100 mm length were cut from the molded plates with 12.7 mm × 12.7 mm fiberglass end tabs affixed using cyanoacrylate adhesive (Loctite, 401). The samples were tested at 2.0 mm min<sup>-1</sup> until failure on an MTS 858 hydraulic load frame with a 25 kN load cell with true strain measurements taken over a gauge length of 25.4 mm using an extensometer. Injection-molded samples were tested according to the ASTM D638 standard at 1 mm min<sup>-1</sup> on an MTS 312 hydraulic load frame with a 25 kN load cell with strain measured using digital image correlation (DIC). Dual 9 MP cameras acquired images for 3D correlation using Vic-3D (Correlated Solutions) during the test. The acquisition rate was chosen based on the test time to acquire roughly 200 images per sample, ranging from 2–10 Hz for the samples with the greatest to least total deformation. Statistical analysis of the tensile testing results was undertaken to identify significant differences in the resulting properties. The two-sample t-test was used to evaluate the observed differences in tensile strength, modulus, and strain-to-failure between each sample set.

### Microstructure analysis method

The microstructure of the molded composites was analyzed using optical and SEM. For optical microscopy, failed tensile specimens were cut at least 5 mm from the failure region, embedded in mounting

epoxy, and polished. The cross-sections were then imaged using an optical microscope (Keyence, VHX-7000) capable of automatically stitching large areas. Example micrographs are available in the Supplementary Section 6. The resulting global fiber and void volume fraction were calculated as described in the authors' prior work<sup>21</sup>. The degree of inhomogeneity in the composites was evaluated following the work of Yourdkhani and Hubert<sup>22</sup>. A binary image of the composite was operated on, from which the distance from each matrix phase pixel to its nearest fiber phase pixel was calculated. The average distance was then compared to that of an idealized homogeneous microstructure represented by a hexagonal array of fibers packed to the same fiber volume fraction. The resulting dispersion index, DI, was calculated as:

$$DI = \frac{\mu}{\mu_i} \quad (4)$$

with a minimum value of 1.0 representing perfect dispersion. Failed specimen fracture surfaces were evaluated using SEM. Samples were gold-sputtered and then scanned at 5 kV accelerating voltage (Zeiss, Auriga). SEM imaging provided qualitative evaluation of the failure modes in the composites.

### DATA AVAILABILITY

The datasets used and/or analyzed during the current study are available from the corresponding author upon reasonable request.

Received: 4 October 2023; Accepted: 6 January 2024;  
Published online: 11 March 2024

### REFERENCES

- Perry, N., Bernard, A., Laroche, F. & Pompidou, S. Improving design for recycling - application to composites. *CIRP Ann. Manuf. Technol.* **61**, 151–154 (2012).
- Zhang, J., Chevali, V. S., Wang, H. & Wang, C. H. Current status of carbon fibre and carbon fibre composites recycling. *Compos. Part B Eng.* **193**, 108053 (2020).
- Utekar, S., SuriyaV, K., More, N. & Rao, A. Comprehensive study of recycling of thermosetting polymer composites—driving force, challenges and methods. *Compos. Part B Eng.* **207**, 108596 (2021).
- Pimenta, S. & Pinho, S. T. Recycling carbon fibre reinforced polymers for structural applications: technology review and market outlook. *Waste Manag.* **31**, 378–392 (2011).
- Meng, F., McKechnie, J. & Pickering, S. J. An assessment of financial viability of recycled carbon fibre in automotive applications. *Compos. Part A Appl. Sci. Manuf.* **109**, 207–220 (2018).
- Colucci, G., Ostrovskaya, O., Frache, A., Martorana, B. & Badini, C. The effect of mechanical recycling on the microstructure and properties of PA6. 6 composites reinforced with carbon fibers. *J. Appl. Polym. Sci.* **132**, 1–9 (2015).

7. Pietrolungo, M., Padovano, E., Frache, A. & Badini, C. Mechanical recycling of an end-of-life automotive composite component. *Sustain. Mater. Technol.* **23**, e00143 (2020).
8. Schinner, G., Brandt, J. & Richter, H. Recycling carbon-fiber-reinforced thermoplastic composites. *J. Thermoplast. Compos. Mater.* **9**, 239–245 (1996).
9. Halpin, J. C. & Kardos, J. L. Strength of discontinuous reinforced composites: I. Fiber reinforced composites. *Polym. Eng. Sci.* **18**, 496–504 (1978).
10. Moothoo, J., Bar, M. & Ouagne, P. Mechanical properties of compression moulded aggregate-reinforced thermoplastic composite scrap. *J. Compos. Sci.* **5**, 299 (2021).
11. Vincent, G. A. et al. Characterisation and improvement of the quality of mixing of recycled thermoplastic composites. *Compos. Part C Open Access* **4**, 100108 (2021).
12. Vincent, G. A. et al. Shredding and sieving thermoplastic composite scrap: method development and analyses of the fibre length distributions. *Compos. Part B Eng.* **176**, 107197 (2019).
13. Barnett, P. R., Gilbert, C. L. & Penumadu, D. Repurposed/recycled discontinuous carbon fiber organosheet development and composite properties. *Compos. Part C Open Access* **4**, 100092 (2021).
14. Rahate, A. S., Nemade, K. R. & Waghuley, S. A. Polyphenylene sulfide (PPS): State of the art and applications. *Rev. Chem. Eng.* **29**, 471–489 (2013).
15. Desio, G. P. & Rebenfeld, L. Crystallization of fiber-reinforced poly (phenylene sulfide) composites. 1. Experimental studies of crystallization rates and morphology. *J. Appl. Polym. Sci.* **44**, 1989–2001 (1992).
16. Barnett, P. R., Young, S. A., Chawla, V., Foster, D. M. & Penumadu, D. Thermo-mechanical characterization of discontinuous recycled/repurposed carbon fiber reinforced thermoplastic organosheet composites. *J. Compos. Mater.* <https://doi.org/10.1177/00219983211015721> (2021).
17. U.S. Energy Information Administration. Electric Power Monthly Report October 2023. [https://www.eia.gov/electricity/monthly/current\\_month/epm.pdf](https://www.eia.gov/electricity/monthly/current_month/epm.pdf) (2023).
18. Rybicka, J., Tiwari, A. & Leeke, G. A. Technology readiness level assessment of composites recycling technologies. *J. Clean. Prod.* **112**, 1001–1012 (2016).
19. Ghossein, H., Hassen, A. A., Paquit, V., Love, L. J. & Vaidya, U. K. Innovative method for enhancing carbon fibers dispersion in wet-laid nonwovens. *Mater. Today Commun.* **17**, 100–108 (2018).
20. Spruiell, J. E., Janke, C. J., Case, S. W. & Reifnider, K. L. A review of the measurement and development of crystallinity and its relation to properties in neat PPS and its fiber reinforced composites. U.S. Department of Energy. <https://doi.org/10.2172/885940> (2004).
21. Barnett, P. R., Young, S. A., Patel, N. J. & Penumadu, D. Prediction of strength and modulus of discontinuous carbon fiber composites considering stochastic microstructure. *Compos. Sci. Technol.* **211**, 108857 (2021).
22. Yourdkhani, M. & Hubert, P. Quantitative dispersion analysis of inclusions in polymer composites. *ACS Appl. Mater. Interfaces* **5**, 35–41 (2013).

## ACKNOWLEDGEMENTS

This research was performed in part while Philip Barnett held an NRC Research Associateship award at the Air Force Laboratory. Nadim Hmeidat would like to acknowledge partial support by the US Department of Energy, Office of Energy Efficiency and Renewable Energy, Advanced Manufacturing Office, under contract DE-AC05-00OR22725 with UT-Battelle, LLC. The authors would like to thank Justin Brackenridge supported by the Strategic Ohio Council for Higher Education, for his assistance in preparing and testing injection-molded specimens, Anthony Pelton of

UES, Inc., for his assistance in thermal characterization, Stephen Pupilampu supported by UTK, for his assistance with SEM imaging, and Ethan Barnhill supported by UTK for his assistance with fiber length measurements. The authors would also like to thank Uday Vaidya of UTK for providing access to the hammer mill and wet-laid machine. Hicham Ghossein of Endeavor Composites is thanked for providing recommended parameters for wet-laid nonwoven production. Ahmed Hassen, supported by ORNL provided the commercial carbon fiber/PPS. Solvay Specialty Polymers graciously provided neat PPS pellets for the injection molding portion of this work. Gen 2 Carbon generously provided recycled carbon fiber nonwovens and precision chopped carbon fibers.

## AUTHOR CONTRIBUTIONS

P.B. and D.P. conceptualized the project. P.B., N.H., and B.Z. developed the methodology and performed experiments. P.B. analyzed the data, wrote the main manuscript text, and edited the manuscript text. N.H., B.Z., and D.P. reviewed the manuscript draft. D.P. provided facilities and financial support for completing the research.

## COMPETING INTERESTS

The authors declare no competing interests.

## ADDITIONAL INFORMATION

**Supplementary information** The online version contains supplementary material available at <https://doi.org/10.1038/s44296-024-00006-y>.

**Correspondence** and requests for materials should be addressed to Philip R. Barnett.

**Reprints and permission information** is available at <http://www.nature.com/reprints>

**Publisher's note** Springer Nature remains neutral with regard to jurisdictional claims in published maps and institutional affiliations.



**Open Access** This article is licensed under a Creative Commons Attribution 4.0 International License, which permits use, sharing, adaptation, distribution and reproduction in any medium or format, as long as you give appropriate credit to the original author(s) and the source, provide a link to the Creative Commons license, and indicate if changes were made. The images or other third party material in this article are included in the article's Creative Commons license, unless indicated otherwise in a credit line to the material. If material is not included in the article's Creative Commons license and your intended use is not permitted by statutory regulation or exceeds the permitted use, you will need to obtain permission directly from the copyright holder. To view a copy of this license, visit <http://creativecommons.org/licenses/by/4.0/>.

© The Author(s) 2024